Diagramas de Fase

Permiten un prediseño de la experiencia

Permiten una explicación inicial de los resultados y/o indican los caminos para modificarlos

Los diagramas de fases pueden ser :

Temperatura - Composición (en general a p.atm.)
Temperatura - Presión
Presión - Composición

VICENTE MUÑOZ SANJOSÉ

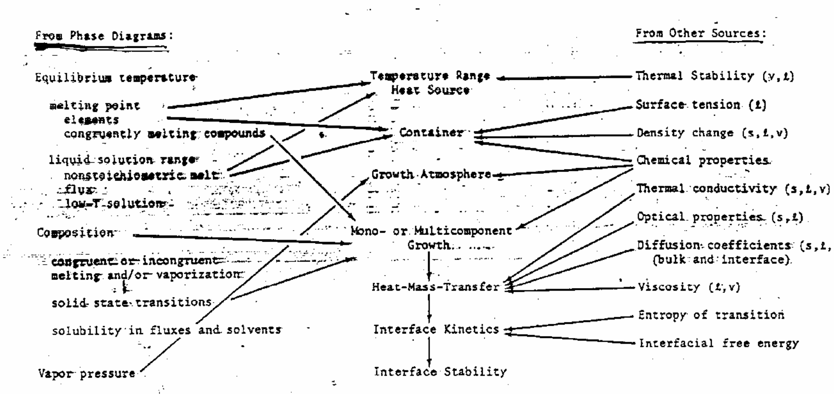

Fig.4.1. Material parameters important for the selection of a crystal growth method, and their relation to growth meters (center column) (s: solid, ℓ: liquid, v: vapor)

Disponibilidad

VICENTE MUÑOZ SANJOSÉ

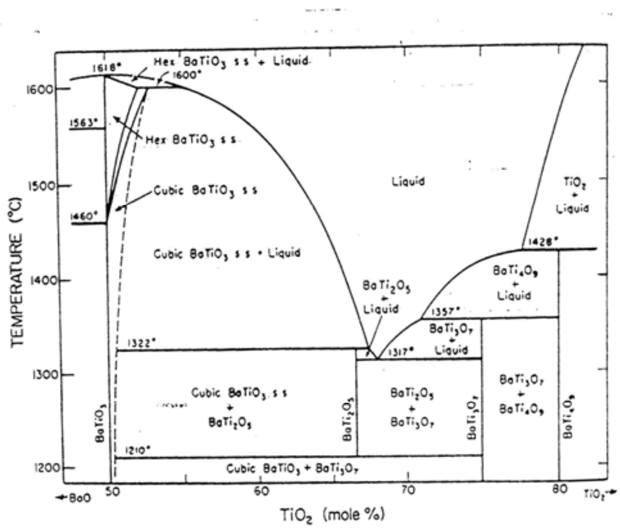

Fig.4.15. Section of phase diagram of BaO-TiO_2 system. From [4.14] by permission of Pergamon Press

VICENTE MUÑOZ SANJOSÉ

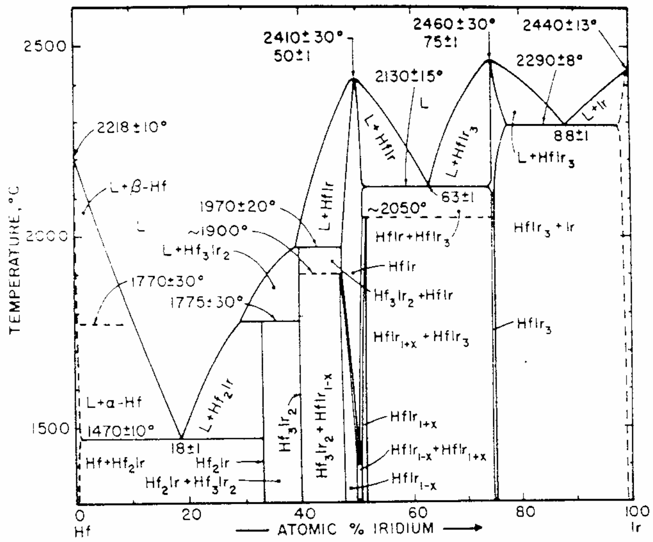

Figure 12. Phase diagram for the system Hf-Ir illustrating types of compounds (from Rudy, 1969).

VICENTE MUÑOZ SANJOSÉ

Simple Binary Phase Diagrams

W.B. White, Phase equilibria

The simplest bi… …olid solubility

Nickel and copp… …ery rules for the formatio…

Since copper a… …neter a two phase mixt…

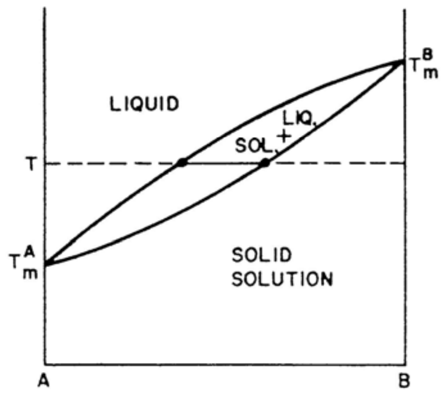

Figure 6. Schematic binary phase diagram for a system with complete miscibility in liquid and solid phases.

The binary diagram

0 → % Cu 100

VICENTE MUÑOZ SANJOSÉ

More Complex Phase Diagrams

W.B. White, Phase equilibria 31

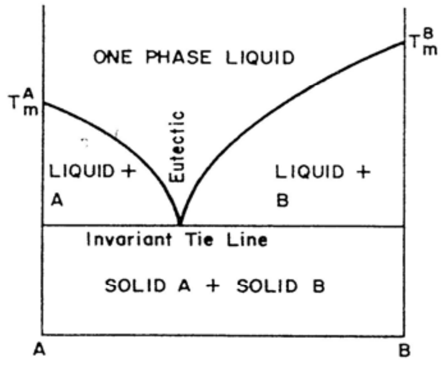

Figure 7. Schematic phase diagram for a system with complete miscibility in the liquid phase and complete immiscibility in the solid phase.

VICENTE MUÑOZ SANJOSÉ

Algunos casos significativos.
Aplicaciones y consideraciones generales

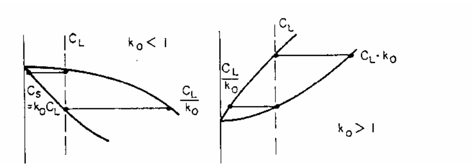

442

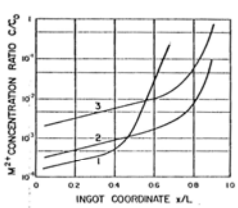

Fig.6.31. Impurity concentration profiles in zone refined KCl ingots. C_0 is the initial impurity level of about 1 ppm. After [6.50]. (1): Polycrystalline ingot. (L = 28cm, l = 1cm, n = 20). Higher purity in front part due to ultra-pure graphite container, lower purity in rear due to horizontal boat arrangement allowing for vapor transfer. (2): Single crystal. (L = 16.5cm, l = 1.5cm, n = 23). Somewhat lower purity in front from quartz container. Higher efficiency in rear from reduction of vapor transfer in vertical arrangement that is also more advantageous for single crystal growth. (3): Identical to (2) except for chlorine bubble formation at growing interface

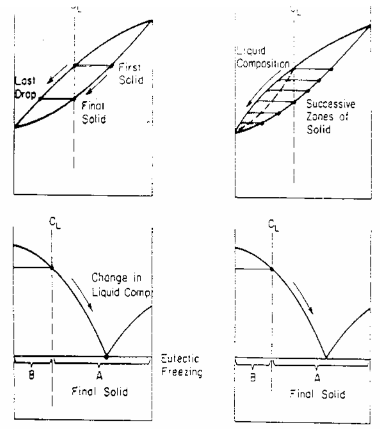

Figure 22. Schematic diagrams illustrating ideal equilibrium cooling and fractionation cooling. Arrows indicate direction of change of liquid composition.

VICENTE MUÑOZ SANJOSÉ

Algunos casos significativos. Aplicaciones y consideraciones generales

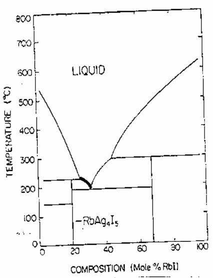

Fig.4.10. Phase diagram for the RbI-AgI system. After [4.11a]

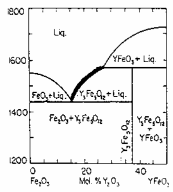

Fig.4.11. Partial phase diagram of the Fe_2O_3-$YFeO_3$ system. From [4.3] by permission of Academic Press

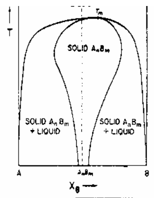

Fig.4.4. Schematic temperature-composition diagram for a compound-forming system A-B. Temperature dependence of the A_nB_m existence range

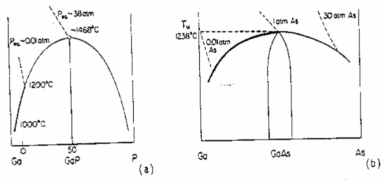

Fig.4.8. T-X projections of the phase figure for (a) the Ga-P system and (b) greatly expanded center portion of the Ga-As system. From [4.3] by permission of Academic Press

VICENTE MUÑOZ SANJOSÉ

Algunos casos significativos. Aplicaciones y consideraciones generales

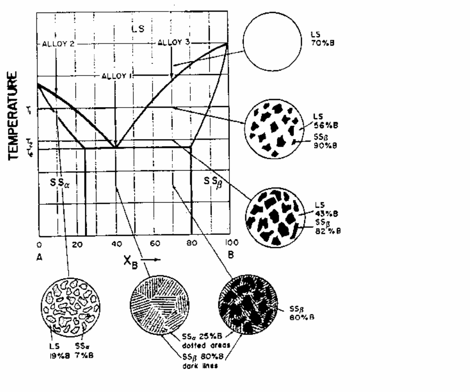

Fig.3.23. Three different solidification processes in a simplified eutectic system (solvus lines drawn vertically) and their structural results. (LS: liquid solution SS: solid solution)

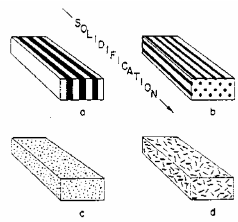

Fig.3.24. Schematic illustration of various eutectic structures: (a) lamellar; (b) rodlike; (c) globular (d) acicular. After [3.22]

equilibrium with a melt of 19% B in A. Their relative amounts follow from the lever rule, (3.26).

VICENTE MUÑOZ SANJOSÉ

Algunos casos significativos. Aplicaciones y consideraciones generales

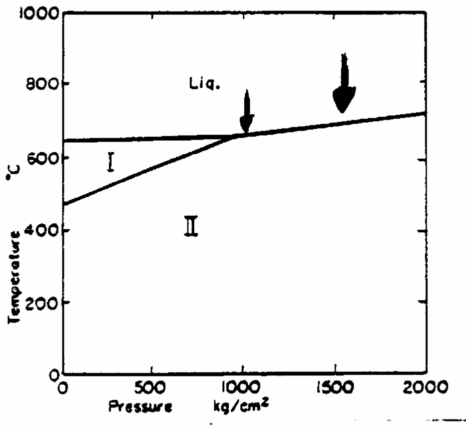

Fig.4.17. P-T phase diagram of CsCl. From [4.17] by permission of North Holland Publ. Co.

VICENTE MUÑOZ SANJOSÉ

Algunos casos significativos. Aplicaciones y consideraciones generales

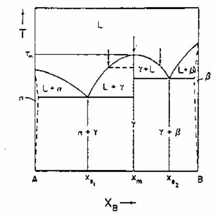

Fig.3.34. Congruently melting compound (composition X_m) in binary phase diagram with two eutectics

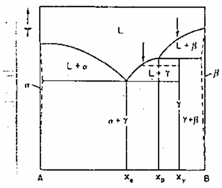

Fig.3.35. Incongruently melting interme-

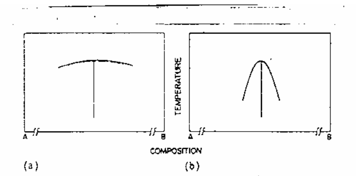

VICENTE MUÑOZ SANJOSÉ

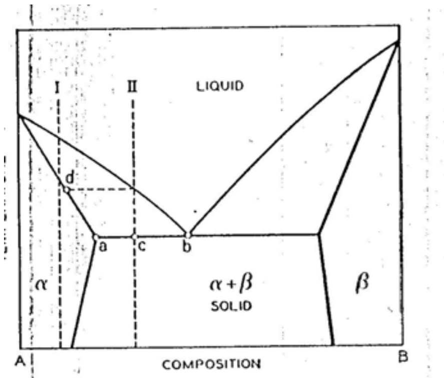

'ig.6.32. Zone refining of eutectic. From [6.37] by permission of John Wiley
ınd Sons

VICENTE MUÑOZ SANJOSÉ

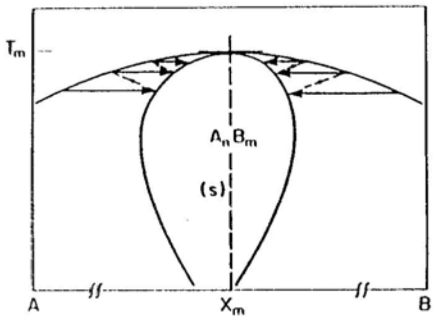

Fig.6.33. Expanded part of binary phase diagram with compound formation. Successive "purification" of off-stoichiometric material by zone melting

VICENTE MUÑOZ SANJOSÉ

.

Método de Bridgman

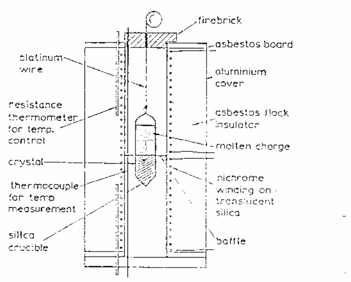

Fig. 1.1. The Bridgman technique. Apparatus of the type shown has been used with a wide range of materials with melting points up to about 1200 C. For higher melting materials, other crucibles and furnace windings can be used. Typical rates of lowering are in the range 5 to 100 mm hr^{-1}.

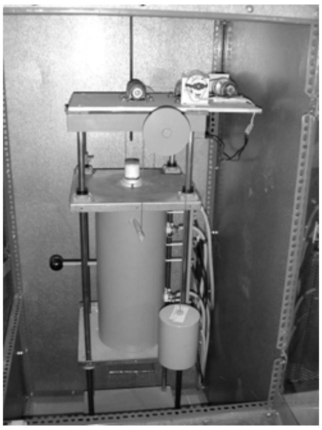

VICENTE MUÑOZ SANJOSÉ

Diagrama de fases del In-Se

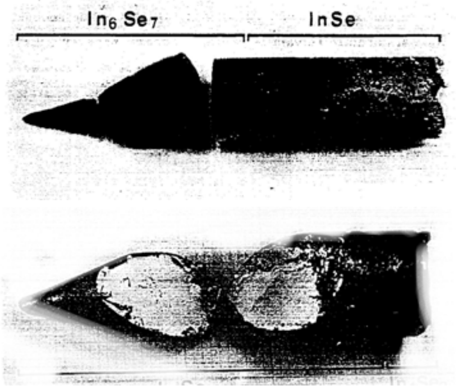

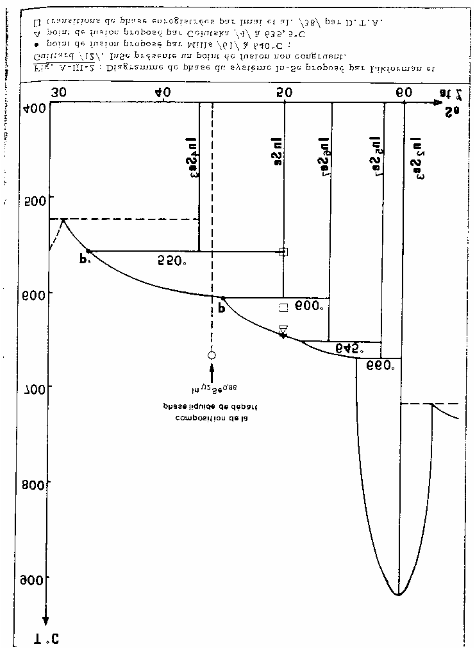

VICENTE MUÑOZ SANJOSÉ

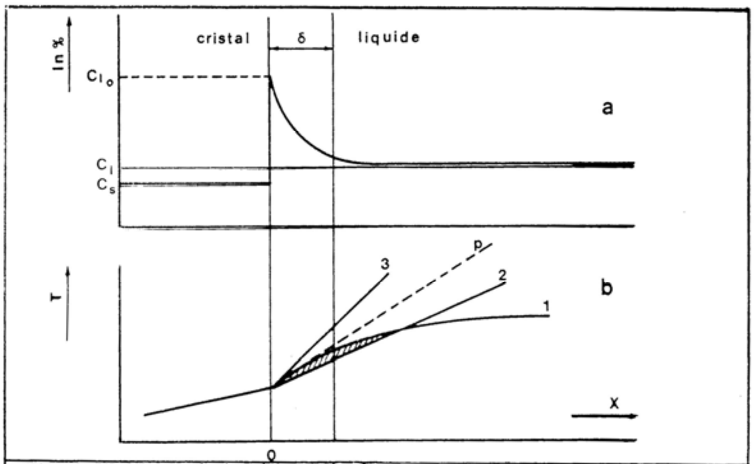

Fig. A-III-15 : Surfusion de constitution :
a - le rejet d'une impureté augmente la concentration de celle-ci au niveau de l'interface solide-liquide ;
b - l'existence de la couche limite peut placer le liquide en surfusion suivant la valeur du gradient thermique réel à l'interface.

VICENTE MUÑOZ SANJOSÉ

Semiconductores laminares III-VI

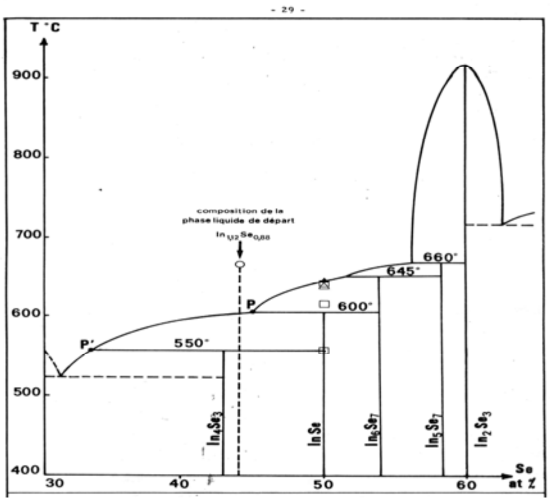

Método Bridgman

VICENTE MUÑOZ SANJOSÉ

Semiconductores laminares III-VI

InSe

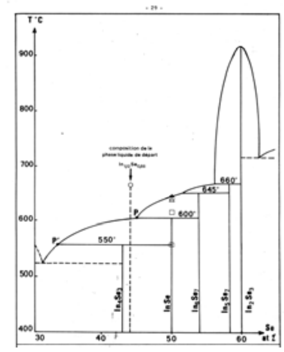

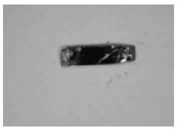

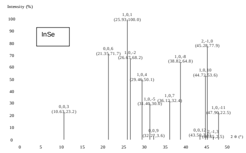

Método Bridgman

VICENTE MUÑOZ SANJOSÉ

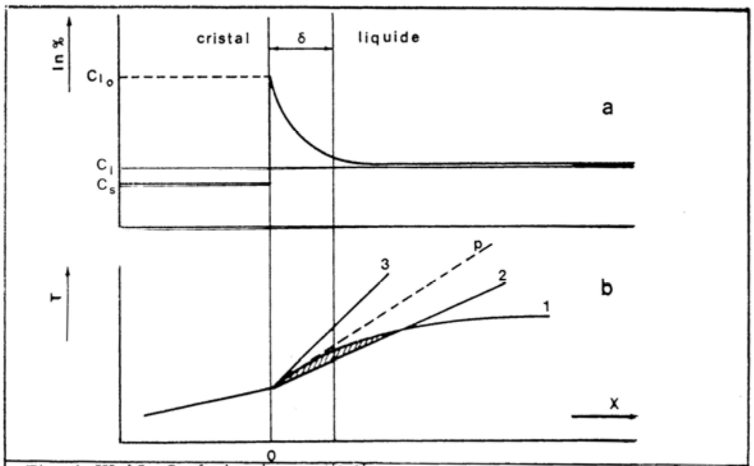

Fig. A-III-15 : Surfusion de constitution :
a - le rejet d'une impureté augmente la concentration de celle-ci au niveau de l'interface solide-liquide ;
b - l'existence de la couche limite peut placer le liquide en surfusion suivant la valeur du gradient thermique réel à l'interface.

VICENTE MUÑOZ SANJOSÉ

428

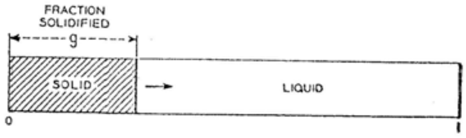

Fig.6.14. Solidification by normal freezing. From [6.37] by permission of John Wiley and Sons

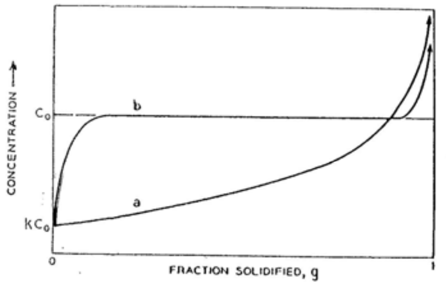

Fig.6.15. Concentration of solute after normal freezing versus fraction solidified for $k < 1$: (a) partial mixing in liquid, (b) transport in liquid by diffusion only. From [6.37] by permission of John Wiley and Sons

VICENTE MUÑOZ SANJOSÉ

429

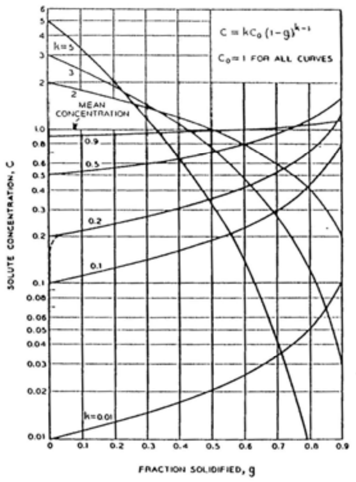

Fig.6.16. Concentration profiles in solid for normal freezing calculated from (6.45) for various effective segregation coefficients k. From [6.37] by permission of John Wiley and Sons

VICENTE MUÑOZ SANJOSÉ

Semiconductores laminares III-VI

GaSe **GaS** **GaTe**

Método Bridgman

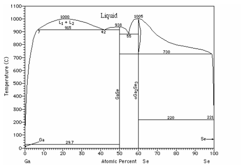

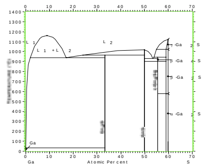

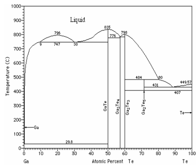

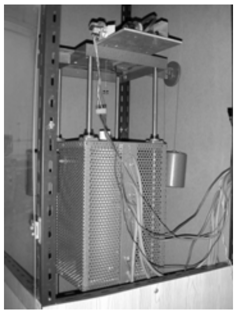

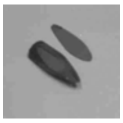

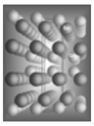

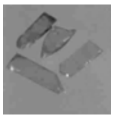

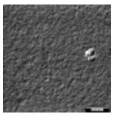

VICENTE MUÑOZ SANJOSÉ

Diagrama de fases Zn-P

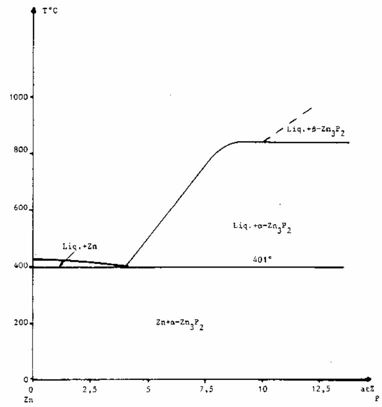

Figure 2: Diagramme de phase du système Zn-P obtenu par Ugai /5/.

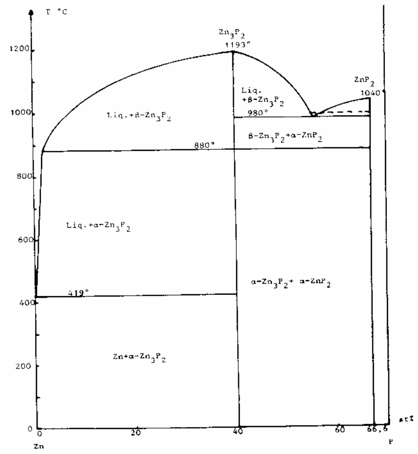

Figure 1: Diagramme de phase du système Zn-P obtenu par Berak /4/.

VICENTE MUÑOZ SANJOSÉ

Crecimiento cristalino y caracterización de materiales semiconductores

Zn_3P_2

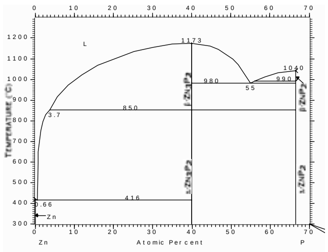

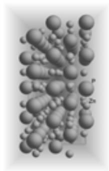

PVT

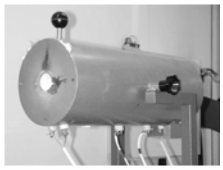

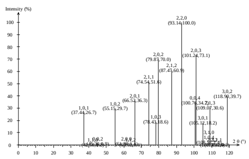

Bridgman no estequiométrico

VICENTE MUÑOZ SANJOSÉ

Diagrama de fases Cd-Te

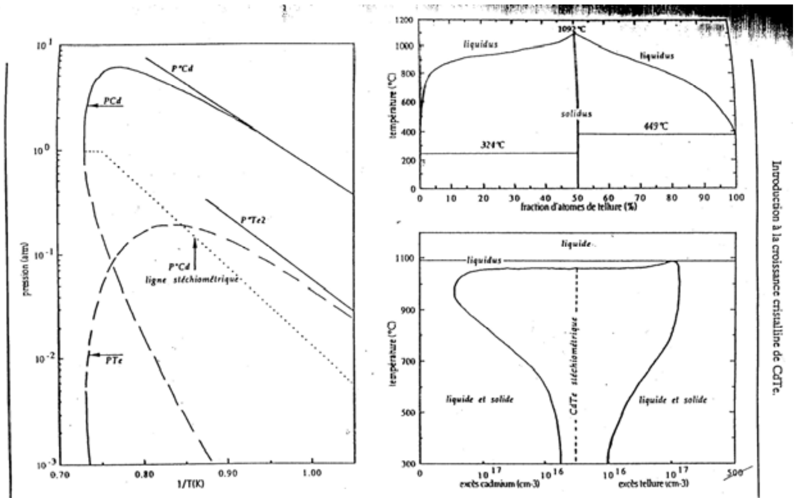

Fig 1.1: diagrammes de phase du tellurure de cadmium.
a-diagramme pression-température entre les trois phases solide-liquide vapeur (nous y avons représenté la pression de cadmium correspondant à un équilibre entre la vapeur et le CdTe solide stéchiométrique).
b,c- diagrammes composition-température (d'après K.Zanio ref 2, page 3).

VICENTE MUÑOZ SANJOSÉ

Diagrama de fases Cd-Te

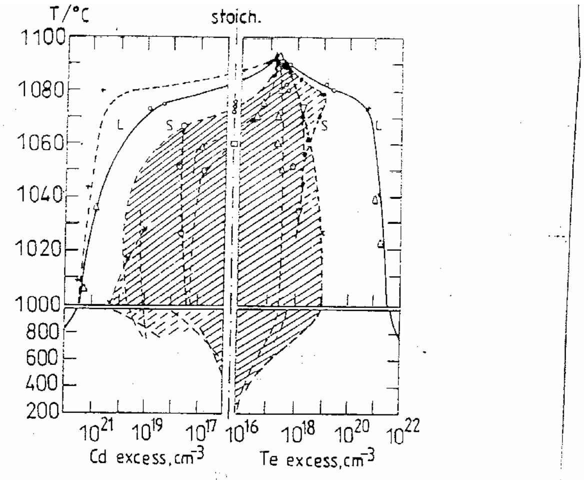

Fig.2.2. The homogeneity region of CdTe in the T-y projection near the melt temperature and below 1000°C (The data are taken from Ref.[6,7,24,35,105] and Ivanov (o) [private communication 1993])

VICENTE MUÑOZ SANJOSÉ

Diagrama de fases Cd-Te

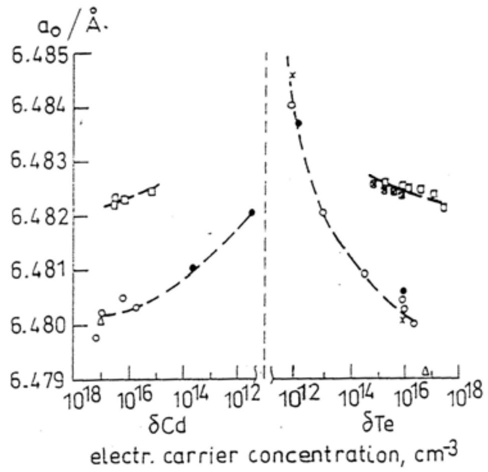

Fig.2.3. The composition dependence of the CdTe lattice parameter a_o taken from Kalushnaja and Kiseleva [36] (○ ●), Song Wen-Bin *et al.*[40] (x) and Wienecke *et al.*[35] (□)

VICENTE MUÑOZ SANJOSÉ

Diagrama de fases Cd-Te

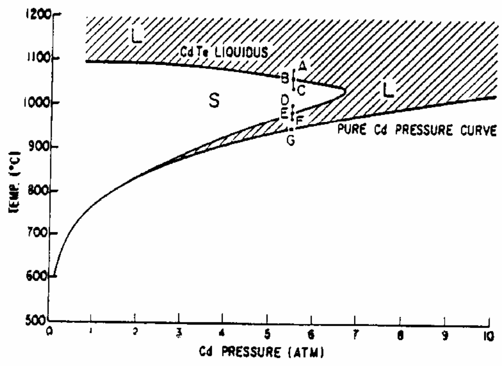

Fig.4.18. T-P projection of the "Cd-rich half" of the Cd-Te system. From [4.18] by permission of the American Institute of Physics

VICENTE MUÑOZ SANJOSÉ

Materiales II-VI

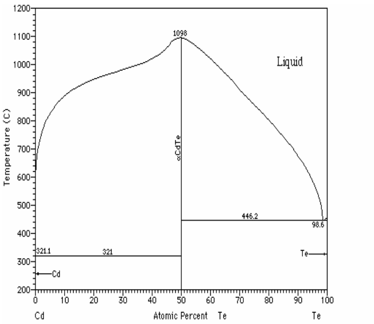

CdTe

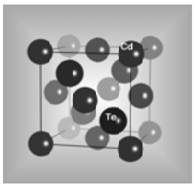

Método Bridgman

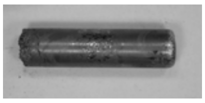

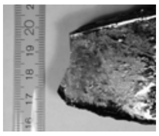

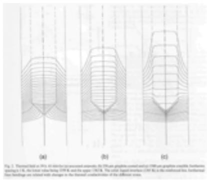

VICENTE MUÑOZ SANJOSÉ